International Journal of GEOMATE, Nov., 2024 Vol.27, Issue 123, pp.108-117
ISSN: 2186-2982 (P), 2186-2990 (O), Japan, DOI: https://doi.org/10.21660/2024.123.4717
Geotechnique, Construction Materials and Environment

# COMPARATIVE ANALYSIS OF LIQUEFACTION POTENTIAL USING THE SWEDISH WEIGHT SOUNDING TEST (SWST) AND N-SPT

Aristya Putra Purba[1], *Hary Christady Hardiyatmo[1] and Ahmad Rifa'i[1]

[1]Department of Civil and Environmental Engineering, Universitas Gadjah Mada, Indonesia

*Corresponding Author, Received: 12 Sep. 2024, Revised: 04 Oct. 2024, Accepted: 10 Oct. 2024

**ABSTRACT:** The assessment of liquefaction potential is an essential aspect of geotechnical engineering. However, the conventional Standard Penetration Test (SPT) often presents logistical and practical challenges, particularly in remote and inaccessible areas. As a result, there is growing interest in alternative methods, such as the Swedish Weight Sounding Test (SWST), which offers a more practical and economical approach to soil characterization. This study uses SWST and SPT to conduct a comparative analysis of liquefaction potential in the Gumbasa irrigation area, specifically in Petobo and Jono Oge, which are susceptible to earthquake-induced liquefaction. Two approaches were used, converting SWST data into equivalent SPT values through empirical correlations and directly utilizing SWST values to estimate liquefaction resistance, which were then compared to SPT-based procedures. In Petobo, the liquefaction resistance derived from empirical correlations shows a 7.18% difference, while the direct SWST approach yields resistance values 1.6 to 2.4 times higher than those from the SPT method. In Jono Oge, significant variations in liquefaction resistance were observed due to differences in soil resistance from the two techniques. However, in the topsoil, a minor gap of 1.54% was observed compared to the SPT method while using empirical correlations. The direct SWST method yielded values 0.87 to 1.48 times higher than those from the SPT. Overall, SWST shows promise for evaluating shallow liquefaction, though additional testing may be necessary for deeper layers. SWST can be a valuable and cost-effective method for preliminary liquefaction assessments, especially in areas where SPT is logistically challenging or expensive.

*Keywords: Swedish Weight Sounding Test, Standard Penetration Test, Liquefaction, Petobo, Jono Oge*

## 1. INTRODUCTION

In geotechnical engineering, soil investigation is essential for accurately understanding subsurface conditions. Therefore, several factors need to be considered. According to [1], the minimum number of soil investigations required depends on the specific type of construction. For instance, canal projects require soil investigations every 50 to 200 meters. Moreover, as outlined in [2], soil investigations must be completed before building permits can be issued for construction projects. However, in practice, budget constraints often make it difficult to fully conduct these investigations.

The Standard Penetration Test (SPT) is a widely adopted technique for in-situ soil sampling. It effectively determines soil properties through empirical correlations or by analyzing samples in the laboratory. Parameters obtained from SPT play a critical role in foundation design and in assessing liquefaction potential [3,4]. However, the test is often costly in terms of mobilization and execution [5], and it requires precise control of the energy applied to the test rods [6]. Considering these limitations, the Swedish Weight Sounding Test (SWST) can serve as either a supplementary or alternative method to SPT.

The International Society for Soil Mechanics and Foundation Engineering (ISSMFE) has recognized SWST as one of four standard penetration tests, collectively referred to as 'weight sounding test' [7]. The term 'Swedish' originates from its early application in Scandinavia, where it was used by the Swedish State Railways to assess roadbed degradation. SWST has since been standardized in European countries through Eurocode 7 [8] and has seen widespread adoption in Japan, particularly for geotechnical investigations [9]. Its cost-effectiveness, along with the ease of mobilizing equipment and conducting field installations, has led to its use in other countries like the Philippines and Iran [10,11]. A modified version of this method, called the Screw Driving Sounding Test (SDST), has also been implemented in several countries [12].

In Indonesia, the use of SWST is not as widespread as it is in other countries. Although the in-situ 'weight sounding test' is mentioned in the [1], it does not provide detailed explanations like those found in [8]. Since its introduction by a Japanese reconnaissance team as a technique for post-earthquake site inspection in Palu, Indonesian researchers have shown a growing interest in studying the SWST [13-15]. The previous application of SWST was also conducted by a Japanese reconnaissance team to examine damage from earthquake-induced liquefaction during the 1999 earthquake in Adapazari, Turkey [16]. The liquefaction events in Palu and Adapazari share similar geological characteristics. First, these areas are formed by alluvial deposits predominantly composed of sand and silty sand. Second, the liquefaction events were initiated by earthquakes triggered by strike-slip fault activity [17,18].

In addition to the geological contributions that were discussed earlier, [19] states that the susceptibility to liquefaction in Palu is associated with the Gumbasa irrigation channel located on the eastern side of Palu Valley. This canal may have affected shallow groundwater conditions, contributing to the liquefaction in Petobo and Jono Oge [20]. As a result, both new and current irrigation projects need to be aware of the potential hazards generated by earthquakes, since reliquefaction may occur during a subsequent earthquake [21,22].

Following the prior discussion, this study compares SWST and SPT liquefaction potential calculations within the Gumbasa irrigation channel. Previous SPT-based liquefaction potential investigations indicated that the irrigation channel is still a possibility [23,24]. Nevertheless, no study has been published to compare the liquefaction potential results of SWST and SPT around the Gumbasa irrigation channel. In this comparison of liquefaction potential evaluations, the SPT-based procedures [25] will be employed to compare results obtained from SPT values and SWST values converted into equivalent SPT values. Additionally, the liquefaction resistance values, calculated directly from SWST measurements [26,27], will also be used to evaluate the liquefaction potential.

The subsequent sections of this article are organized as follows. Section 2 discusses the research significance. Section 3 describes the study area, focusing on the geological and topographical features of the Gumbasa irrigation region. Section 4 outlines the methodologies for assessing liquefaction potential using SPT and SWST, covering both direct and empirical correlation methods. Section 5 presents and compares the findings, highlighting the liquefaction resistance and safety factor values from both methods in the Petobo and Jono Oge areas. Finally, Section 6 summarizes the main findings and offers directions for future research.

## 2. RESEARCH SIGNIFICANCE

This study provides an updated perspective on liquefaction potential evaluation through cost-effective in-situ testing techniques like SWST. It aims to understand better how SWST can be a feasible alternative by comparing its efficacy and reliability with the commonly used SPT. The results assist geotechnical investigators in making informed decisions, particularly in selecting the most effective techniques for liquefaction potential assessment. Additionally, this study may contribute to SWST-related research in Indonesia, with possible applications in other regions. Furthermore, it can offer valuable insights if SWST is later incorporated into the Indonesian Geotechnical Code.

## 3. STUDY AREA

The study area is located in Petobo and Jono Oge, specifically within the Gumbasa irrigation region. According to [28], this region has a high susceptibility to liquefaction. Soil test results from the SPT and SWST, conducted by a Japanese reconnaissance team at the research site [29], indicate that the entire area lies on alluvial plains (Fig. 1a and Fig. 1b). This ensures that the comparison between the SPT and SWST data is carried out under the same geological conditions.

In addition to geological conditions, the proximity between the SPT and SWST data being compared is carefully considered. According to [1], every soil investigation for the canal project must be conducted at intervals of 50 to 200 meters. This range is selected to prevent significant variations in the land attributes being compared, ensuring that the results remain consistent. Accordingly, two suitable SPT and SWST datasets, which met these criteria for distance and geological consistency, were selected for analysis, as shown in Fig. 1c and Fig. 1d.

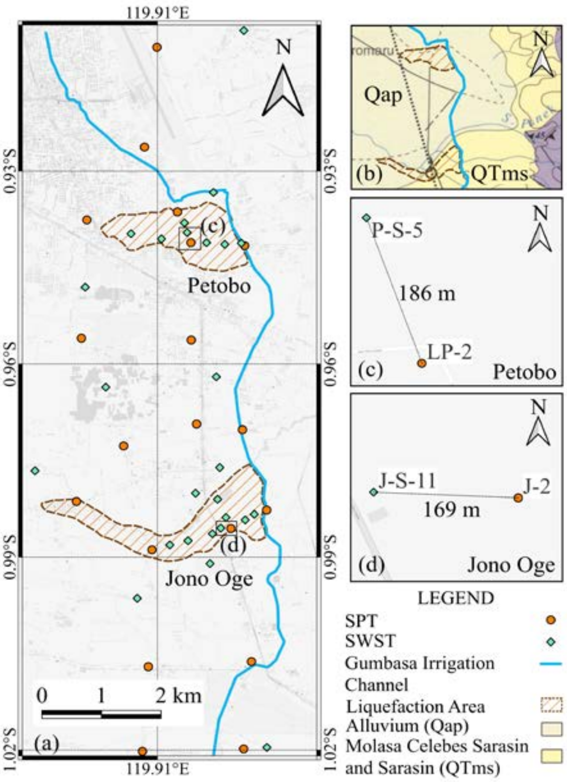


Fig. 1 (a) Spatial distribution of SPT and SWST, (b) Geological conditions at the research location modified [30], (c) and (d) Two sets of data were selected based on the distance to the soil investigation points

Since this soil investigation serves as the basis for reconstructing the Gumbasa irrigation channel, it is important to consider the limitation of the SWST method, which can only investigate soil resistance up to a depth of 10 meters [31]. As stated by [1], the canal design requires a minimum soil investigation depth (Zi), as shown in Fig. 2. The Gumbasa irrigation channel to be constructed has typical dimensions of 1.2 meters in width (b) and 1.36 meters in height (h). Moreover, the recommended Zi value for this project is 3.36 meters, which meets the minimum criteria for soil investigation using the SWST method.

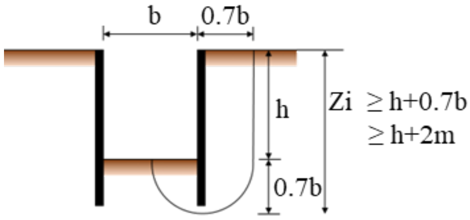


Fig. 2 The minimum depth of soil investigation for canals modified [1]

Considering the objective of this study is to evaluate liquefaction potential using SWST and SPT data, it is essential to examine the distribution of $N_{SPT}$ values measured at the selected boreholes, as shown in Fig. 3.

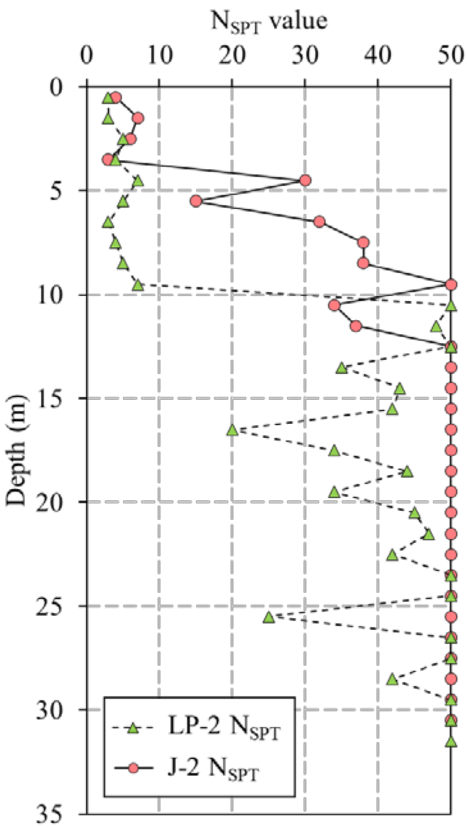


Fig. 3 Distribution of $N_{SPT}$ values for LP-2 and J-2 boreholes

An initial indication of liquefaction potential occurs when the $N_{SPT}$ value is below 10 at depths of up to 10 meters [32]. A low $N_{SPT}$ value is directly correlated with relative density [25], with land subsidence caused by liquefaction increasing as relative density decreases [33]. Furthermore, [34] found that the critical depth for liquefaction rarely exceeds 12 meters. This is consistent with a study by [20], which observed liquefaction events in Palu at depths between 2 and 4 meters below the ground surface, evidenced by post-liquefaction ground subsidence. Given this understanding, SPT data can serve as comparative data for assessing liquefaction potential, while also considering the depth limitations of the SWST method in soil investigation.

## 4. METHODS

### 4.1 Evaluation of Liquefaction Potential Using the SPT Approach

Based on [1], the SPT-based liquefaction potential method is performed by carefully applying the method proposed by [25], which is developed by the original version proposed by [34]. The original method was previously used by [35] to assess the liquefaction potential at two selected locations. The safety factor ($FS_{liq}$) is determined by dividing the cyclic resistance ratio (CRR) by the cyclic stress ratio (CSR) to assess the probability of liquefaction. The soil profile at a particular depth can potentially liquefy if $FS_{liq} < 1$.

#### *4.1.1 CSR triggered by seismic activity*

At a specific depth, z, the seismic activity can trigger a cyclic stress ratio (CSR) in the soil profile, representing a uniform equivalent value equal to 65% of the peak cyclic shear stress ratio. The peak shear stress can be determined using the approach explained in [34], as expressed in Eq. (1).

$$CSR_{M,\sigma'_v} = 0.65\frac{\tau_{max}}{\sigma'_v} = 0.65\,\frac{\sigma_v}{\sigma'_v}\frac{a_{max}}{g}\,r_d \quad (1)$$

Where $\tau_{max}$ refers to the peak shear stress induced by an earthquake, $\sigma'_v$ denotes the effective vertical stress, $\sigma_v$ represents to the total vertical stress at a specific depth (z), $a_{max}/g$ mean the peak horizontal acceleration (as a ratio of gravity) at the ground surface, and $r_d$ represents the reduction factor for shear stress that takes into consideration the dynamic response of the soil profile. The expression for the parameter $r_d$ can be found in Eq. (2) to Eq. (4).

$$r_d = \exp[\,\alpha(z) + \beta(z) \cdot M\,] \quad (2)$$

$$\alpha(z) = -1.012 - 1.126\sin\left(\frac{z}{11.73} + 5.133\right) \quad (3)$$

$$\beta(z) = 0.106 - 0.118\sin\left(\frac{z}{11.28} + 5.142\right) \quad (4)$$

The parameters z and M denote the subsurface depth in meters and the earthquake's magnitude, respectively, while the unit of measurement for the sine arguments is radians.

The method defined in [36] accurately calculate the peak horizontal acceleration at the ground surface, denoted as $a_{max}$. It begins with carefully identifying the site class by taking into account the average field standard penetration resistance, denoted as $\bar{N}$. The measurement extends to a depth of 30 meters from the ground surface and is determined using Eq. (5).

$$\bar{N} = \frac{\sum_{i=1}^{n} d_i}{\sum_{i=1}^{n} d_i / N_i} \quad (5)$$

Where $\sum_{i=1}^{n} d_i$ denotes the total thickness of the soil layers within the top 30 meters, and $N_i$ is the measurement penetration resistance in the specific depth. To obtain the value of $a_{max}$, the following equation is applied, as shown in Eq. (6).

$$a_{max} = F_{PGA} \cdot PGA \quad (6)$$

The local site effect coefficient, expressed as $F_{PGA}$ in Table 1, represents the effect of local site conditions amplification of peak ground acceleration (PGA). PGA refers to earthquakes recorded in 2018 that caused liquefaction in Palu [37].

Table 1. Local site effect coefficient modified [36]

| $\bar{N}$ | Site Class | PGA ≤0.1 | PGA =0.2 | PGA =0.3 | PGA =0.4 | PGA =0.5 | PGA ≥0.6 |
|---|---|---|---|---|---|---|---|
| N/A | SA | 0.8 | 0.8 | 0.8 | 0.8 | 0.8 | 0.8 |
| N/A | SB | 0.9 | 0.9 | 0.9 | 0.9 | 0.9 | 0.9 |
| >50 | SC | 1.3 | 1.2 | 1.2 | 1.2 | 1.2 | 1.2 |
| 15 - 50 | SD | 1.6 | 1.4 | 1.3 | 1.2 | 1.1 | 1.1 |
| <15 | SE | 2.4 | 1.9 | 1.6 | 1.4 | 1.2 | 1.1 |
| - | SF | requires specific geotechnical investigations and site-specific response analysis | | | | | |

*Note: N/A is Not Applicable.*

*4.1.2 CRR of soil in the specific depth*

The CRR of the soil is affected by the number of shaking cycles, which is related to the earthquake magnitude scaling factor (MSF) and the effective overburden stress, represented by the index $K_\sigma$. In addition, the correlation for CRR is calculated by using a reference magnitude (M) of 7.5 and an effective vertical stress ($\sigma'_v$) of 1 atm. This correlation is then modified for other values of M and $\sigma'_v$ using the method outlined in Eq. (7) to Eq. (15).

$$CRR_{M,\sigma'_v} = CRR_{M=7.5,\ \sigma'_v=1} \cdot MSF \cdot K_\sigma \quad (7)$$

$$CRR_{M=7.5,\ \sigma'_v=1} = \exp\left(\frac{(N_1)_{60cs}}{14.1} + \left(\frac{(N_1)_{60cs}}{126}\right)^2 - \left(\frac{(N_1)_{60cs}}{23.6}\right)^3 + \left(\frac{(N_1)_{60cs}}{25.4}\right)^4 - 2.8\right) \quad (8)$$

$$MSF = 6.9 \exp\left(\frac{-M}{4}\right) - 0.058 \leq 1.8 \quad (9)$$

$$K_\sigma = 1 - C_\sigma \ln\left(\frac{\sigma'_v}{P_a}\right) \leq 1.1 \quad (10)$$

$$C_\sigma = \frac{1}{18.9 - 2.55\sqrt{(N_1)_{60cs}}} \leq 0.3 \quad (11)$$

$$(N_1)_{60cs} = (N_1)_{60} + \Delta(N_1)_{60} \quad (12)$$

$$(N_1)_{60} = N_{SPT}\, C_E\, C_B\, C_R\, C_S\, C_N \quad (13)$$

$$C_N = \left(\frac{P_a}{\sigma'_v}\right)^{0.784 - 0.0768\sqrt{(N_1)_{60cs}}} \leq 1.7 \quad (14)$$

$$\Delta(N_1)_{60} = \exp\left(1.63 + \frac{9.7}{FC+0.01} - \left(\frac{15.7}{FC+0.01}\right)^2\right) \quad (15)$$

Where $CRR_{M=7.5,\ \sigma'_v=1}$ denotes the CRR for an earthquake of magnitude 7.5 and an effective vertical stress of 1 atm. The value of the magnitude scaling factor is denoted as MSF, and the overburden correction factor is written as $K_\sigma$. The $(N_1)_{60cs}$ value represents SPT blow counts, which have been carefully corrected for several key parameters in order to enhance the accuracy of the analysis. These parameters include the earthquake magnitude (M), and calibration factors, $\Delta(N_1)_{60}$, $C_E$, $C_B$, $C_R$, $C_S$, $C_N$, which are used to account for various factors such as fines content correction, hammer energy ratio, diameter of borehole, rod length, sample tube, and overburden pressure, respectively. A value of $P_a$ represents air pressure in kPa, $\sigma'_v$ represents vertical effective stress, and FC is the fines content of the soil expressed as a percentage.

## 4.2 Evaluation of Liquefaction Potential Using the SWST Approach

Two different approaches can be employed to analyze liquefaction potential using SWST; (1) the SPT-based approach, which specifically involves converting the SWST data ($N_{SW}$) to $N_{SPT}$ values, and (2) directly utilizing the SWST data. Each of these approaches yields a CRR value needed to estimate liquefaction safety factor, $FS_{liq}$. However, the CSR value is still consistently determined by Eq. (1).

*4.2.1 CRR from estimated $N_{SPT}$ values*

An empirical correlation between $N_{SW}$ and $N_{SPT}$ was originally proposed by Inada (1960) based on field data collected from highway construction sites in Nagoya and Osaka, Japan [38]. Inada's correlation is calculated using Eq. (16).

$$N_{SPT} = 2W_{SW} + 0.067N_{SW} \quad (16)$$

Where $W_{SW}$ represents the weight required for penetration in kN, and $N_{SW}$ represents the number of half turns required to reach a rod penetration of 0.25 meters (ht/m).

Furthermore, [38] determined an empirical correlation considering the influence of grain composition, as formulated in Eq. (17) and Eq. (18).

$$N_{SPT} = \frac{\sqrt{e_{max} - e_{min}}}{10}(N_{sw} + 40 \times W_{sw}) \quad (17)$$

$$e_{max} - e_{min} = 0.23 + 0.06/D_{50} \quad (18)$$

Where $e_{max} - e_{min}$ is a formula developed by [39], and $D_{50}$ as the mean grain size in milimeters (mm).

Moreover, the CRR value can be determined by integrating Eq. (7) to Eq. (15) and applying the estimated $N_{SPT}$ value obtained from Eq. (16) and Eq. (17). Then, the CRR will be divided by the CSR from Eq. (1) to determine the $FS_{liq}$ value.

*4.2.2 CRR from $N_{SW}$ values (direct approach)*

The direct approach is applied to SWST without using soil samples. The equation given by [26] applies to two soil types; (1) sand, and (2) sand with silt and silty sand.

For clean sand (FC < 5%), the CRR is given by Eq. (19).

$$CRR = 0.016\sqrt{N'_{sw1}} \quad (19)$$

For sand with silt (5% ≤ FC < 15%) and silty sand (FC ≥ 15%), the CRR is given by Eq. (20). The value of $N'_{sw1}$ can be determined using Eq. (21).

$$CRR = 0.02\sqrt{N'_{sw1}} \quad (20)$$

$$N'_{sw1} = (N_{sw} + 40 \times W_{sw})\sqrt{\frac{98}{\sigma'_v}} = N'_{sw}\sqrt{\frac{98}{\sigma'_v}} \quad (21)$$

The values of $N'_{sw1}$ are determined by accounting for the effects of static penetration and effective confining stress. FC represents the fines content, $W_{SW}$ is measured in kN, and $\sigma'_v$ is measured in kPa.

When adequate soil samples are collected and the fines content at each layer is determined, the influence of fines can be incorporated into the assessment of liquefaction resistance from SWST using the Eq. (22) proposed by [27].

$$CRR = \alpha_{sw}\sqrt{N'_{sw1}} + \beta_{sw}\sqrt{FC} \quad (22)$$

Where FC is expressed as a percentage, and $\alpha_{sw}$ and $\beta_{sw}$ are parameters that change with FC as follows; $\alpha_{sw}$ is 0.016 and $\beta_{sw}$ is 0 for clean sand (FC < 5%), $\alpha_{sw}$ is 0.02 and $\beta_{sw}$ is 0 for sand with fines (5% ≤ FC < 15%), $\alpha_{sw}$ is 0.02 and $\beta_{sw}$ is 0.016 for silty sand and silt (FC ≥ 15%).

## 5. RESULTS AND DISCUSSION

The selection of two sets of SPT and SWST data was based on the similarity of geological characteristics and the distance between investigation locations in the Petobo and Jono Oge areas, which are historical liquefaction sites. Table 2 and Table 3 show the soil profiles for each data sets.

Table 2. The Petobo area data set (Fig. 1c)

| In-Situ Test | SPT | | SWST | |
|---|---|---|---|---|
| Label | LP-2 | | P-S-5 | |
| GWL (m) | 3.09 | | 1.5 | |
| Depth (m) | USCS | $N_{SPT}$ | $W_{SW}$ (kg) | $N_{SW}$ (ht/m) |
| 0.5 | CL | 3 | 25 | 8 |
| 1 | CL | 3 | 25 | 8 |
| 1.5 | CL | 3 | 50 | 56 |
| 2 | CL | 3 | 50 | 4 |
| 2.5 | CL | 5 | 50 | 12 |
| 3 | SC | 4 | 50 | 64 |
| 3.5 | SC | 4 | 100 | 72 |
| 4 | SC | 4 | 100 | 40 |
| 4.5 | CL | 7 | 100 | 24 |
| 5 | CL | 7 | 100 | 36 |
| 5.5 | CL | 5 | 100 | 124 |
| 6 | CL | 5 | 100 | 52 |
| 6.25 | CL | 5 | 100 | 68 |

*Note: CL. silty clay, SC. Clayey-sands.*

Table 3. The Jono Oge area data set (Fig. 1d)

| In-Situ Test | SPT | | SWST | |
|---|---|---|---|---|
| Label | J-2 | | J-S-11 | |
| GWL (m) | 2.7 | | 0.5 | |
| Depth (m) | USCS | $N_{SPT}$ | $W_{SW}$ (kg) | $N_{SW}$ (ht/m) |
| 0.5 | CL-ML | 4 | 25 | 4 |
| 1 | SM-SC | 7 | 25 | 12 |
| 1.5 | SM-SC | 7 | 25 | 12 |
| 2 | SM-SC | 7 | 50 | 176 |
| 2.5 | CH | 6 | 50 | 144 |
| 3 | CH | 6 | 100 | 80 |
| 3.5 | CL | 3 | 100 | 64 |
| 4 | CL | 3 | 100 | 84 |
| 4.5 | SW | 30 | 100 | 72 |
| 5 | SW | 30 | 100 | 36 |
| 5.5 | SP | 15 | 100 | 64 |
| 6 | SP | 15 | 100 | 32 |
| 6.5 | SP | 32 | 100 | 92 |
| 7 | SP | 32 | 100 | 40 |
| 7.5 | SW | 38 | 100 | 56 |
| 8 | SW | 38 | 100 | 40 |
| 8.5 | SW | 38 | 100 | 272 |
| 9 | SW | 38 | 100 | 160 |

*Note: CL-ML. silty clay-silty fine sands, SM-SC. silty sand-clayey sands, CH. fat clays, CL. silty clay, SW. well-graded sands, SP. poorly-graded sands.*

In the Petobo area, there is a spatial separation of 186 meters between the SPT test labeled LP-2 and the SWST test labeled P-S-5 (Fig. 1c). Meanwhile, in the Jono Oge area, the SPT test labeled J-2 and the SWST test labeled J-S-11 have a separation distance of 169 meters (Fig. 1d). The soil depth to be evaluated is adjusted based on the depth of the SWST observations, and the highest groundwater level (GWL) between the two tests is selected for evaluating the liquefaction potential [40].

### 5.1 Analysis of the Petobo Area

*5.1.1 Comparison between $N_{SPT}$ and estimated $N_{SPT}$ from the Petobo area*

A comparative analysis of SPT and SWST data sets in the Petobo area was conducted using the empirical correlation suggested by Inada (1960) and [38]. However, the results from both empirical correlations may not differ significantly (Fig. 4).

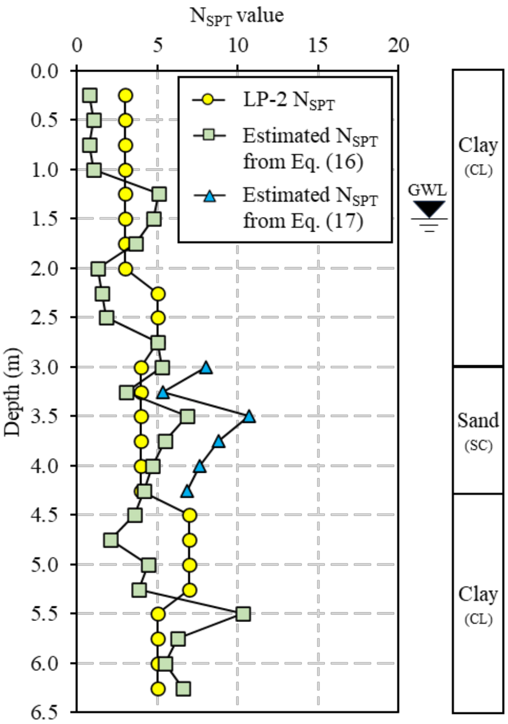


Fig. 4 Comparison $N_{SPT}$ from the Petobo area

From Fig. 4, the correlation estimated by Inada (1960) provides a better fit when compared to the average $N_{SPT}$ values for all types of soil. The average $N_{SPT}$ value for all soil types up to a depth of 6.25 m at the LP-2 borehole is 4.4, while the value estimated using Inada's equation is 4.0. The empirical correlation proposed by [38], however, is not applicable due to its limited relevance to cohesionless soils.

Moreover, when considering the average $N_{SPT}$ value specifically for cohesionless soils, the $N_{SPT}$ value for the LP-2 borehole is 4.0. The correlation values estimated using Inada's equation and [38] are 4.9 and 7.9, respectively. The correlation proposed by Inada appears to be more reliable than that proposed by [38] for cohesionless soils in the Petobo area.

*5.1.2 Comparison of CRR and $FS_{liq}$ between the estimated and direct approaches from the Petobo area*

The comparison of CRR values determined from SPT, SPT correlations, and SWST shows that these values are similar (Fig. 5). CRR values were calculated for layers of cohesionless soil using the procedure defined by [25]. Based on the average CRR value at borehole LP-2, the estimated values for SPT Estimated-1 (Inada's equation), SPT Estimated-2 [38], Direct-1 [26], and Direct-2 [27] are 0.14, 0.15, 0.18, 0.22, and 0.32, respectively. The CRR resulting from Inada's empirical correlation is similar to the CRR value obtained through SPT. However, the direct approach using SWST data yields results that are significantly different.

CSR calculations were initially conducted using Eq. (1) to estimate liquefaction potential. The CSR value should account for the effects of the local site, as calculated by Eq. (5) and Eq. (6). As shown in Table 1, the results of Eq. (5) for determining the site class in the Petobo area indicate that the area is classified as SE site class. By identifying the site class, the $a_{max}$ value for the Petobo area is 0.47 g, considering the local site effects. The liquefaction potential assessment using the SPT-based procedures shows a range of liquefaction depths from 3 to 4.25 meters (Fig. 5).

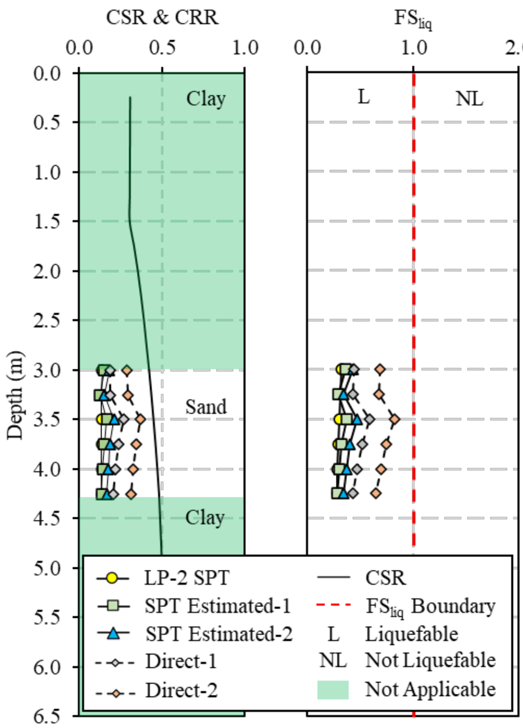


Fig. 5 Comparison CRR and $FS_{liq}$ from the Petobo area

The analysis of $FS_{liq}$ results showed a correlation between the CRR and CSR values, indicating that both the SPT and SWST procedures were correlated with the SPT values and produced the same liquefaction depth. However, the average $FS_{liq}$ values obtained from borehole LP-2, SPT Estimated-1 (Inada's equation), SPT Estimated-2 [38], Direct-1 [26], and Direct-2 [27] were 0.30, 0.32, 0.40, 0.48, and 0.72, respectively. The $FS_{liq}$ value derived from estimating the CRR using Inada's equation was the most comparable to the SPT-based approach. Furthermore, the direct SWST approach resulted in a higher $FS_{liq}$ value due to the greater liquefaction resistance.

## 5.2 Analysis of the Jono Oge Area

### *5.2.1 Comparison between $N_{SPT}$ and estimated $N_{SPT}$ from the Jono Oge area*

Similar to a previous study conducted in the Petobo area, a comparison has been made between the original SPT data and the SWST data (Fig. 6), which were converted into SPT values using the empirical correlation proposed by Inada (1960) and [38].

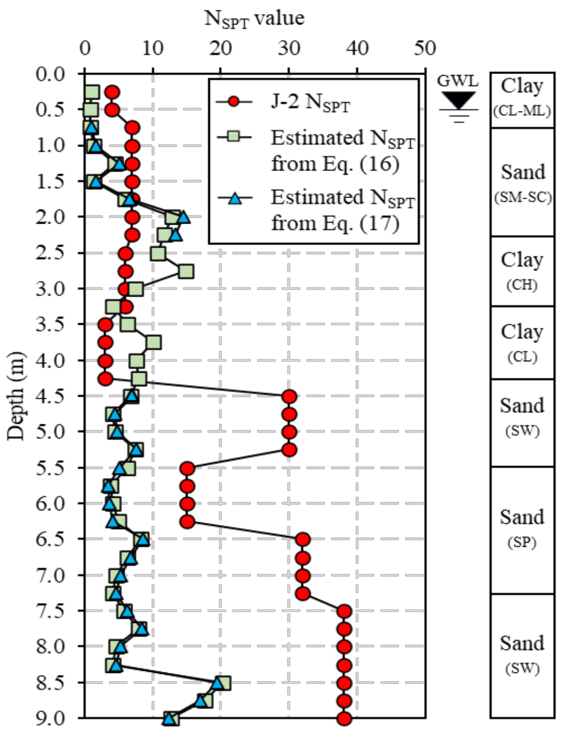


Fig. 6 Comparison $N_{SPT}$ from the Jono Oge area

The data presented in Fig. 6 reveals a significant discrepancy across the depth range of 4.5 to 9 meters. This difference arises because the SPT values increase rapidly from a depth of 4.5 meters, whereas the SWST values remain relatively constant up to 9 meters. According to borehole J-2, the average $N_{SPT}$ value for all soil types is 18.03; however, Inada's equation yields a value of 6.68. For the cohesionless soil layer, the average $N_{SPT}$ value is 23.96, while the $N_{SPT}$ values derived from the Inada's equation and [38] are 6.79 and 7.03, respectively. If such significant differences exist, additional soil investigations may be required to validate the soil resistance in the actual conditions.

### *5.2.2 Comparison of CRR and $FS_{liq}$ between the estimated and direct approaches from the Jono Oge area*

An analysis of CRR values obtained from SPT, SPT correlations, and SWST reveals that these values are generally comparable, except at depths ranging from 4.5 to 5.25 meters and 6.5 to 9 meters (Fig. 7). It can be shown that certain soil layers at specific depths may be susceptible to liquefaction, while others may not [41]. These findings are consistent with the earlier discussion, which indicated an increase in $N_{SPT}$ values at depths between 4.5 and 9 meters. However, at depths between 5.5 and 6.25 meters, the CRR value was low due to the $N_{SPT}$ value being below 20, indicating a potential for liquefaction [34].

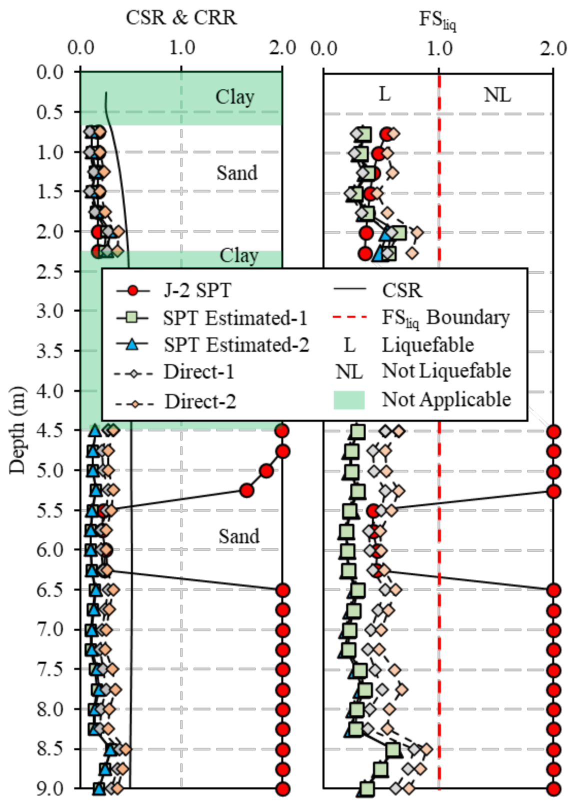


Fig. 7 Comparison CRR and $FS_{liq}$ from the Jono Oge area

After adjusting the $a_{max}$ value for the local site effect, the CSR value required for assessing liquefaction potential was determined. Based on the estimated results from Eq. (5), the Jono Oge area is classified as an SD site class (Table 1). This particular site class is in better condition than the site class in the Petobo area. The difference may be related to the geological differences in Petobo and Jono Oge (Fig. 1b). The $a_{max}$ value in the Jono Oge area is 0.38 g.

Due to the uniformity in $N_{SPT}$ values at depths ranging from 4.5 to 9 meters, the comparison of $FS_{liq}$ values will focus on the range of 0.75 to 2.25 meters, where the data is more consistent. The average $FS_{liq}$ values were found to be 0.42, 0.38, 0.41, 0.37, and 0.62 for borehole J-2, SPT Estimated-1 (Inada's equation), SPT Estimated-2 [38], Direct-1 [26], and Direct-2 [27], respectively. The $FS_{liq}$ value provided by [38] closely matches the $FS_{liq}$ value obtained from the SPT-based procedures. Similar to the analysis conducted in the Petobo area, the $FS_{liq}$ values show the greatest variation when applying the direct SWST method proposed by [27].

## 6. CONCLUSIONS

This study conducted a comparative analysis of liquefaction potential using the SWST and SPT methods at two locations, Petobo and Jono Oge. Based on the soil resistance, the average $N_{SPT}$ values for all soil types in the Petobo area, derived from SPT data, is 4.4, which closely matches the estimates based on Inada's correlation for SWST data, at 4.0. These results suggest that the correlation between SWST and empirical formulas can provide reliable estimates of soil resistance. However, notable differences were observed at depths beyond 4.5 meters in the Jono Oge area, where the average $N_{SPT}$ measured using SPT was 18.03, whereas Inada's correlation only reached 6.68. The observed discrepancies, indicating that SWST may underestimate soil resistance in specific areas, could be due to differences in the distances between investigation points, even though they share the same geological conditions.

For the liquefaction analysis in the Petobo area, the CRR values obtained from the SPT-based procedures, which is 0.14, and the CRR obtained from the correlation using the Inada equation, which is 0.15, show similar results. Consequently, the $FS_{liq}$ calculated by the two approaches reveals a slight gap of 7.18% in the $FS_{liq}$ derived from the SPT approach. In contrast, the $FS_{liq}$ derived from the SWST direct method shows greater significance due to the higher CRR value. The $FS_{liq}$ value generated by the SWST direct method is 1.6 to 2.4 times greater than the $FS_{liq}$ value generated by the SPT method.

For the liquefaction analysis in the Jono Oge area, the CRR results showed significant variation beyond 4.5 meters due to a substantial increase in soil resistance based on the SPT test. However, when assessing liquefaction potential considering the uniform topsoil, the average $FS_{liq}$ value derived from the correlation formula proposed by [38] shows a minor gap of 1.54% compared to the $FS_{liq}$ derived from the SPT-based procedures. In contrast, the SWST direct method produces a higher $FS_{liq}$ value than the SPT method, with a range of 0.87 to 1.48.

The findings suggest that the SWST approach can be a valuable tool for the preliminary evaluation of liquefaction, particularly in areas where conducting SPT testing may pose logistical challenges. When the SWST overestimates liquefaction resistance at greater depths, such as in Jono Oge, it is recommended to combine SWST with additional in-situ testing, such as SPT. Further research is suggested to enhance the reliability of SWST correlations, especially for deeper soil strata and locations with complex stratigraphy.

## 7. ACKNOWLEDGMENTS

The authors would like to express their gratitude to the Indonesian Ministry of Public Works and Public Housing, particularly the River Basin Management Office of Sulawesi III, for their valuable support in providing the necessary data for this research. Their contribution was critical in enabling the completion of this study.

## 8. REFERENCES

[1] National Standardization Agency of Indonesia, Geotechnical Design Requirements, SNI 8460:2017, Jakarta, 2017.

[2] Government of Indonesia, Regulation of the Government of the Republic of Indonesia Number 16 of 2021 on the Implementation of Law Number 28 of 2002 Concerning Buildings, Jakarta, 2021.

[3] Putra R.R., Relationship Between Obtained Ultimate Bearing Capacity Results Based on N-SPT Results and Static Load Tests, International Journal of GEOMATE, Vol. 19, Issue 74, 2020, pp.153-160.

[4] Zakariya A., Rifa'i A., and Ismanti S., The Correlation of Liquefaction Potential With Excess Pore Water Pressure in Kretek 2 Bridge Area Using Empirical and Numerical Methods, Journal of the Civil Engineering Forum, Vol. 10, Issue 1, 2024, pp.39-48.

[5] Marto A., Sakai G., Suemasa N., Mohd Yunus N.Z., Jusoh S.N., Ahmad K., and Mohd Satar M.H., Screw Driving Sounding Test; A New Technology in Soil Investigation Work Particularly for Soft Soil, MATEC Web of Conferences, Vol. 276, 2019, pp.1-13.

[6] Anbazhagan P., Ayush K., Yadhunandan M.E., Siriwanth K., Suryanarayana K., and Sahodar G., Effective Use of SPT Hammer Energy Measurement and Integrated Subsurface Investigation, Indian Geotechnical Journal, Vol. 52, Issue 5, 2022, pp.1079-1096.

[7] International Society for Soil Mechanics and Foundation Engineering, Report of the ISSMFE Technical Committee on Penetration Testing of Soils - TC 16 With Reference Test Procedures, Swedish Geotechnical Society, 1984.

[8] European Committee for Standardization, Eurocode 7 - Geotechnical Design - Part 2: Ground Investigation and Testing, prEN 1997-2:2007, Brussels, 2007.

[9] Tsukamoto Y., Ishihara K., Kawabe S., and Kanemitsu S., Liquefaction-Induced Road Embankment Failures, Proceedings of the Institution of Civil Engineers, Forensic Engineering, Vol. 166, Issue FE2, 2013, pp.64-71.

[10] Armario M.J.P., Follosco M.P.V., Gargullo J.M.B., Lu P.A.R., and Luna R.A.C., Swedish Weight Sounding Test: Site Investigation for a Solar Power Facility in the Philippines, Smart Geotechnics for Smart Societies, 2023, pp.2060-2065.

[11] Habibi M., Cheshomi A., and Fakher A., A Case Study of Liquefaction Assessment Using Swedish Weight Sounding, Proceedings of the 4th International Conference on Earthquake Engineering, Taipei, Taiwan, 2006, Paper No. 038.

[12] Soralump S., Shah A., Chaithong T., Sakai G., and Boonyatee T., Soil Strength Estimation Using Screw Driving Sounding Technique for Bangkok Clay Layers, International Journal of GEOMATE, Vol. 25, Issue 111, 2023, pp.193-201.

[13] Irdhiani, Rifa'i A., Fathani T.F., and Adi A.D., Post-Earthquake Liquefaction Vulnerability Mapping by Swedish Weight Sounding and Standard Penetration Test, Civil Engineering Journal, Vol. 10, No. 07, July, 2024, pp.2216-2232.

[14] Setiawan H., Rahmatika U.I., and Ramadhani S., Liquefaction Potential Based on Swedish Weight Sounding Test in Langaleso Village, Sigy Regency, International Journal of Innovative Science and Research Technology, Vol. 8, Issue 4, 2023, pp.302-309.

[15] Setiawan H., Ilaiya I., Oktaviana I.S., Irdhiani, Fadliah I., and Hasanah Y., The Study of Liquefied Soil by Using Swedish Weight Sounding Test in Jono Oge Village, Sigi Regency, IOP Conference Series: Earth and Environmental Science, Vol. 1075, 2022, pp.1-14.

[16] Ansal A., Recent Advances in Earthquake Geotechnical Engineering and Microzonation, Kluwer Academic Publishers, 2004, pp. 1-354.

[17] GEER, HATTI, and PuSGen, Geotechnical Extreme Events Reconnaissance: The 28 September 2018 M7.5 Palu-Donggala, Indonesia Earthquake, Research Institute for Housing and Human Settlements Ministry of Public Works and Housing Republic of Indonesia, 2019, pp.1-74.

[18] Mollamahmutoglu M., Kayabali K., Beyaz T., and Kolay E., Liquefaction-Related Building Damage in Adapazari During the Turkey Earthquake of August 17, 1999, Engineering Geology, Vol. 67, 2003, pp.297-307.

[19] Watkinson I.M. and Hall R., Impact of Communal Irrigation on the 2018 Palu Earthquake-Triggered Landslides, Nature Geoscience, Vol. 12, Issue 11, 2019, pp.1-11.

[20] Kiyota T., Furuichi H., Hidayat R.F., Tada N., and Nawir H., Overview of Long-Distance Flow-Slide Caused by the 2018 Sulawesi Earthquake, Indonesia, Soils and Foundations, Vol. 60, Issue 3, 2020, pp.722-735.

[21] Cummins P.R., Irrigation and the Palu Landslides, Nature Geoscience, Vol. 12, 2019, pp.881-882.

[22] Bradley K., Mallick R., Andikagumi H., Hubbard J., Meilianda E., Switzer A., Du N., Brocard G., Alfian D., Benazir, Feng G., Yun S.H., Majewski J., Wei S., and Hill E.M., Earthquake-Triggered 2018 Palu Valley Landslides Enabled by Wet Rice Cultivation, Nature Geoscience, Vol. 12, 2019, pp.935-940.

[23] Sauri S., Rifa'i A., and Hardiyatmo H.C., Liquefaction Vulnerability Analysis Using N-SPT Value and Grain Size Analysis on Gumbasa Irrigation Canal in the Post-Disaster Petobo Area, Sulawesi, IOP Conference Series: Earth and Environmental Science, Vol. 930, 2021, pp.012081.

[24] Andiny A.N., Faris F., and Adi A.D., Re-Liquefaction Hazard Evaluation in Flow-Slide Affected Area of Jono Oge, Central Sulawesi, Indonesia, IOP Conference Series: Earth and Environmental Science, Vol. 861, 2021, pp.052030.

[25] Idriss I.M. and Boulanger R.W., SPT-Based Liquefaction Triggering Procedures, Report No. UCD/CGM-10/02, Center for Geotechnical Modeling, Department of Civil and Environmental Engineering, University of California, Davis, 2010.

[26] Tsukamoto Y., Hyodo T., and Hashimoto K., Evaluation of Liquefaction Resistance of Soils From Swedish Weight Sounding Tests, Soils and Foundations, Vol. 56, Issue 1, 2016, pp. 74-85.

[27] Tsukamoto Y., Noda S., Nakatsukasa M., and Katayama H., Use of Weight Sounding for Examining the Liquefaction-Induced River Levee Failures, Proceedings of the Institution of Civil Engineers - Geotechnical Engineering, Vol. 1, Issue 40, 2020, pp.1-40.

[28] Buana T.W., Hermawan W., Rahdiana R.N., Widyaningrum R., Wahyudin, Hasibuan G., Wiyono, and Sollu W.P., Atlas of Liquefaction

Susceptibility Zones in Indonesia, Geological Agency, Ministry of Energy and Mineral Resources, 2019.
[29] PT Indra Karya (Persero), Boring Survey for Basic Response for Central Sulawesi Earthquake (Phase 1) Under the JICA Survey for Disaster Information Collection in Indonesia, JICA, 2019.
[30] Sukamto R., Sumadirja H., Suptandar T., Hardjoprawiro S., and Sudana D., Reconnaissance Geological Map of the Palu Quadrangle, Sulawesi, 1973.
[31] Gargullo J.M.B. and Luna R.A.C., Application of Swedish Weight Sounding Test for the Geotechnical Assessment of Solar Power Plant, Proceedings of the 7th International Conference on Geotechnical and Geophysical Site Characterization, Barcelona, 2024, pp.1-40.
[32] Ishihara K., Stability of Natural Deposits During Earthquakes, International Society for Soil Mechanics and Geotechnical Engineering (ISSMGE), 1985.
[33] Fattah M.Y., Salim N.M., and Haleel R.J., Effect of Relative Density on Liquefaction Potential of Sandy Soil from Small Laboratory Machine Foundation Model, International Journal of Science and Research, Vol. 7, No. 1, 2018, pp. 661-672.
[34] Seed H.B. and Idriss I.M., A Simplified Procedure for Evaluating Soil Liquefaction Potential, Earthquake Engineering Research Center, Report No. EERC 70-9, University of California, Berkeley, 1970.
[35] Abdullah H.H., Fattah M.Y., and Abed A.H., Determination of Liquefaction Potential for Two Selected Sites in Kerbala City - Middle of Iraq, International Journal of Engineering & Technology, Vol. 7, No. 1, 2018, pp. 25-32.
[36] National Standardization Agency of Indonesia, Procedures for Earthquake Resistance Planning for Building and Non-Building Structures, SNI 1726:2019, Jakarta, 2019.
[37] Meisei Electric Co. Ltd., Palu Earthquake Strong Motion Waveform by Observation System, Badan Meteorologi, Klimatologi, dan Geofisika (BMKG), 2018.
[38] Tsukamoto Y., Ishihara K., Harada K., and Kanatani M., Correlation Between Penetration Resistance of Swedish Weight Sounding Tests and SPT Blow Counts in Sandy Soils, Journal of Geotechnical and Geoenvironmental Engineering, Vol. 130, Issue 6, 2004, pp.596-606.
[39] Cubrinovski M. and Ishihara K., Maximum and Minimum Void Ratio Characteristics of Sands, Soils and Foundations, Vol. 42, Issue 6, 2002, pp.65-78.
[40] Hardiyatmo H.C., Earthquake Engineering for Structural and Geotechnical Analysis, Gadjah Mada University Press, First Edition, 2022, pp. 1-522.
[41] Fattah M.Y., Salim N.M., and Haleel R.J., Liquefaction Potential of Sandy Soil from Small Laboratory Machine Foundation Model, International Review of Civil Engineering, Vol. 9, No. 1, 2018, pp. 11-19.